

# Overview of Dynamic Models for $\gamma N \rightarrow \Delta$

D. Drechsel and L. Tiator

*Institut für Kernphysik, Universität Mainz, 55099 Mainz, Germany*

**Abstract.** We present an overview of dynamic and related models for pion electroproduction on the nucleon due to  $\Delta(1232)$  excitation. The electromagnetic multipoles and their ratios obtained from these models and from effective field theories are compared, and the existing contradictory results for the pion cloud effects are discussed.

**Keywords:** pion electroproduction, dynamic models, pion cloud, short vs. long distance physics

**PACS:** 11.80.Et, 13.60.Le, 14.20.Gk

## INTRODUCTION

The  $\Delta(1232)$  or  $P_{33}$  is the strongest resonance in the pion ( $\pi$ ) and photon ( $\gamma$ ) induced reactions on the nucleon (N). It is the only isolated resonance of the nucleon, and the Argand diagram of  $\pi$ -N scattering is a perfect circle in the  $\Delta(1232)$  region up to c.m. energies  $W \approx 1400$  MeV. In the framework of a quark model with SU(6) symmetry, the  $\Delta(1232)$  and the nucleon constitute a degenerate ground state of the 3-quark system. This symmetry is broken by a spin-dependent "hyperfine" interaction due to a residual force of the quark-gluon interaction. Because of its spin dependence this interaction also leads to a tensor force, which yields non-spherical (D state) components in the wave functions. Whereas the photoexcitation process  $\gamma + N \rightarrow \Delta(1232)$  is dominated by a magnetic dipole transition (M1), these D states give rise to a small electric quadrupole transition (E2). However, the experimental ratio  $R_{EM} = E2/M1 \approx -2.5\%$  can only be reached with an unnaturally large bag radius of about 1 fm. It is therefore now generally assumed that a large contribution of the E2 value stems from the pion cloud dominating the large-distance physics.

The aspects of short- and long-distance physics were first studied in chiral bag models by describing the nucleon with an interior quark bag of radius  $r_0 \approx 0.5$  fm and a pion cloud extending to radii  $r \approx 1.5$  fm. Since the quadrupole moment scales with  $r^2$ , the break-down in pion cloud and bag contributions depends strongly on the chosen radius  $r_0$ , although the overall size of  $R_{EM}$  is relatively stable and in reasonable agreement with the data. Nowadays the long-range physics is systematically described by effective field theories (EFTs) based on an expansion in the external momenta, the pion mass, and the N- $\Delta$  mass splitting. The effects of the short-distance physics are absorbed in low-energy constants (LECs), defined by the coefficients in front of the most general lagrangians in accordance with QCD. However, the splitting in short- and long-distance physics is still not unique, because it depends on the scale  $\lambda$  used in the renormalization process of the loop integrals.

Another, more phenomenological approach to pion scattering and pion photoproduction is given by dynamic models (DMs). Whereas EFTs are an exact representation of QCD in the sense that they produce a perturbation series based on the most general lagrangian with the symmetries of QCD, a DM starts from a simplified but reasonable lagrangian that is treated to all orders by means of Lippman-Schwinger or similar equations. As a result the two approaches are complementary. Dynamic models nicely describe the  $\pi$ -N scattering in the resonance region and thus yield a unitary scattering amplitude, whereas they have problems with gauge invariance and relativity. On the other hand, EFTs are manifestly Lorentz and gauge invariant, whereas the perturbative approach can not be expected to give a fully unitary amplitude.

Because of its importance in pion scattering and pion photoproduction, the  $\Delta$  is responsible for several ground state properties of the nucleon by sum rules:

- The Adler-Weisberger sum rule connects the axial coupling constant  $g_A$  with an integral over  $\sigma_{tot}^{\pi^+ p} - \sigma_{tot}^{\pi^- p}$ , the difference of the total cross sections for charged pion scattering off the proton. The  $\Delta(1232)$  turns out to be essential to saturate this sum rule.

- The Gerasimov-Drell-Hearn sum rule expresses the square of the anomalous magnetic moment,  $\kappa_N^2$ , by an integral over  $\sigma_{3/2} - \sigma_{1/2}$ , the difference of the helicity dependent total cross sections for photoabsorption on the nucleon. The integral over the  $\Delta(1232)$  region yields the sum rule value within about 10 %.
- According to Fubini, Furlan, and Rossetti, the Pauli form factor  $F_2^N(Q^2)$  is proportional to an integral over the first relativistic structure function for neutral pion electroproduction,  $A_1^{(+,0)}$ . Again, the integral over the  $\Delta(1232)$  region contributes about 90 % to the sum rule value, the remainder being due to dipole absorption near threshold and in the second resonance region.
- Related to the low energy theorem of Nambu, Lourié, and Shrauner, a further theorem of Fubini, Furlan, and Rossetti gives a connection between  $F_1^V(Q^2) - G_A^V(Q^2)$ , the difference of the isovector Dirac and axial form factors, and an integral over the sixth relativistic structure function  $A_6^{(-)}$  for charged pion electroproduction. The relative closeness of the two radii is expressed by the fact that the large positive contribution of the  $\Delta(1232)$  is essentially canceled by large negative contributions mainly from the second resonance region.

In conclusion the structure of the nucleon is intimately interwoven with the properties of the  $\Delta(1232)$ . This also applies to the question whether elementary particles like the nucleon are "intrinsically" spherical or deformed objects. In fact in a simple quark model, the hyperfine tensor force will inevitably admix D-state components to both nucleon and  $\Delta(1232)$  wave functions. In particular, the "deformation" leads to a quadrupole component in the N- $\Delta(1232)$  transition, which will be discussed in the following sections. In principle one could also think about the "reorientation effect"  $\Delta(1232) \rightarrow \gamma + \Delta(1232)$  appearing as an intermediate state in the reaction  $\gamma + N \rightarrow \gamma' + \pi^0 + N'$ . This reaction is presently under investigation at MAMI with the aim to determine the magnetic dipole moment of the  $\Delta(1232)$ , which should take a complex and energy-dependent value due to the finite width of the  $\Delta(1232)$ . However, the electric quadrupole moment has no diagonal value because of parity and time-reversal invariance. It is therefore unlikely that radiative pion photoproduction will ever teach us something about the deformation of the  $\Delta(1232)$  proper, although we expect a sizeable oblate quadrupole moment of the  $\Delta(1232)$ .

## BASICS

### Scattering matrix

Let us recall some basic definitions for the simple case of pion-nucleon scattering below the two-pion threshold and with the approximation that the electromagnetic interaction can be neglected. Because of angular momentum and parity conservation for the strong interaction, the S-matrix is then diagonal in a representation with quantum numbers  $l$  (orbital angular momentum),  $J = l \pm 1/2$  (total angular momentum), and isospin  $I = 1/2$  or  $3/2$ . All the physics is contained in the scattering phases  $\delta_{l\pm}^I(W)$ , where  $W$  is the total energy in the c.m. frame. (Note that we suppress the isospin index  $I$  in most of the following text.) The S-matrix elements are

$$S_{l\pm}(W) = e^{2i\delta_{l\pm}(W)}. \quad (1)$$

The S-matrix is unitary, i.e.,  $S^\dagger(W)S(W) = 1$  and  $S_{l\pm}^*(W)S_{l\pm}(W) = 1$ . Next we define the elements of the T- and K-matrices by

$$S_{l\pm}(W) = 1 + 2iT_{l\pm}(W) = \frac{1 + iK_{l\pm}(W)}{1 - iK_{l\pm}(W)}. \quad (2)$$

These matrix elements can be expressed by the scattering phases,

$$T_{l\pm}(W) = \frac{K_{l\pm}(W)}{1 - iK_{l\pm}(W)} = \sin\delta_{l\pm}(W)e^{i\delta_{l\pm}(W)}, \quad (3)$$

$$K_{l\pm}(W) = \frac{T_{l\pm}(W)}{1 + iT_{l\pm}(W)} = \tan\delta_{l\pm}(W). \quad (4)$$

According to these definitions, the T-matrix is purely imaginary at resonance,  $\delta_{l\pm}(W_R) = \pi/2$ , whereas the K-matrix has a pole at this point. In particular the  $\Delta(1232)$  resonance with quantum numbers  $l = 1, J = 3/2$  leads to a pole,  $K_{1+}(W) \rightarrow \infty$  if  $W \rightarrow 1232$  MeV, whereas  $T_{1+} = i$  in this limit. On the other hand, a resonance is defined by a pole of the S-matrix (or T-matrix) in the complex energy plane, with negative imaginary part of the energy. In particular, the

$\Delta(1232)$  pole lies at  $W_R \approx (1210 - 50i)$  MeV. In case of approximations, which are inevitable in most calculations, it is recommended to approximate the K-matrix elements. As shown by Eq. (2), the S-matrix is unitary for any real value of  $K = V$ , whereas  $T = V$  results in  $S^\dagger S = 1 + 4V^2$  and violates unitarity at second order in the potential.

## Resonances and speed plot

The analytic continuation of a resonant partial wave as function of energy should generally lead to a pole in the lower half-plane of the second Riemann sheet. A pronounced narrow peak reflects a time-delay in the scattering process due to an unstable excited state. This time-delay is related to the speed of the scattering amplitude [1, 2],

$$SP(W) = \left| \frac{dT(W)}{dW} \right|. \quad (5)$$

In the vicinity of the resonance pole, the energy dependence of the full amplitude,  $T(W) = t(W) + T_R(W)$ , is given by the resonance contribution,

$$T_R(W) \rightarrow \frac{Z \Gamma_R}{M_R - W - i\Gamma_R/2}, \quad (6)$$

whereas the background contribution  $t(W)$  should be a smooth function, ideally a constant. The speed has its maximum at  $W = M_R$ ,  $SP(M_R) = H$ , and the half-maximum values are  $SP(M_R \pm \Gamma_R/2) = H/2$ . This yields the pole position of the resonance at  $W = M_R - i\Gamma_R/2$ . The residue of the pole is determined by the resonance pole parameter  $Z$ , which is a complex number with absolute value  $r$  and phase  $\Phi$ . The latter is due to the interference with the background, it may be determined from the phase of the complex speed vector  $dT/dW$  at the pole. The Particle Data Group [3] gives the following residue for pion-nucleon scattering at the position of the  $\Delta(1232)$ :  $r \approx (53 \pm 3)$  MeV/ $\Gamma_R$  and  $\Phi \approx (-47 \pm 1)^\circ$ . In the case of pion photoproduction, the strong interaction takes place only after the resonance excitation, and therefore we may expect a phase rotation of about  $-20^\circ$  to  $-25^\circ$  by the interference between background and resonance.

## Electromagnetic multipoles

We consider the reaction  $\gamma^*(k, \varepsilon) + N(p, s) \rightarrow \pi(q) + N'(p', s')$ , with  $k, p, q$ , and  $p'$  the momenta of the respective particles,  $\varepsilon$  the polarization of the virtual photon  $\gamma^*$ , and  $s$  and  $s'$  the polarization of the nucleon in the initial and final state, respectively. The matrix elements of the transition four-current  $(\rho, \vec{J})$  are classified as transverse electric (E), transverse magnetic (M), longitudinal (L), and Coulomb or "scalar" currents (S). Denoting the isospin with  $I$ , a pion-nucleon state can be excited by 4 multipole transitions,

$$\mathcal{M}_{l\pm}^I(W, Q^2) = (E_{l\pm}^I, M_{l\pm}^I, L_{l\pm}^I, S_{l\pm}^I), \quad (7)$$

with the exception that the multipoles  $M_{0\pm}^I, E_{0-}^I, E_{1-}^I, L_{0-}$  and  $S_{0-}$  do not exist. The longitudinal and Coulomb multipoles are related by gauge invariance,  $\vec{k} \cdot \vec{J} = \omega \rho$ , which leads to

$$|\vec{k}| L_{l\pm}^I(W, Q^2) = \omega S_{l\pm}^I(W, Q^2). \quad (8)$$

Since the photon c.m. energy  $\omega$  vanishes for  $Q^2 = Q_0^2 = W^2 - M^2$ , the longitudinal multipole must have a zero at that momentum transfer,  $L_{l\pm}^I(W, Q_0^2) = 0$ . Furthermore, the longitudinal and Coulomb multipoles have to become equal in the real photon limit,  $L_{l\pm}^I(W, Q^2 = 0) = S_{l\pm}^I(W, Q^2 = 0)$ . Another important property is the model-independent behavior of the multipoles at physical threshold (vanishing pion momentum,  $q = |\vec{q}| = 0$ ) and at pseudothreshold (Sievert limit, vanishing photon momentum  $k = |\vec{k}| = 0$ ):

$$\begin{aligned} (E_{l+}^I, L_{l+}^I) &\rightarrow k^l q^l \quad (l \geq 0) \\ (M_{l+}^I, M_{l-}^I) &\rightarrow k^l q^l \quad (l \geq 1) \\ (L_{1-}^I) &\rightarrow kq \\ (E_{l-}^I, L_{l-}^I) &\rightarrow k^{l-2} q^l \quad (l \geq 2). \end{aligned} \quad (9)$$

According to Eq. (8) the Coulomb amplitudes acquire an additional factor  $k$  at pseudothreshold, i.e.,  $S_{l\pm}^I \sim kL_{l\pm}^I$ . This limit is reached at  $Q^2 = -(W - M)^2$ , and because no direction is defined at  $\vec{k} = 0$ , the electric and longitudinal multipoles have to be related at this point,

$$E_{l+}^I/L_{l+}^I \rightarrow 1 \text{ and } E_{l-}^I/L_{l-}^I \rightarrow -l/(l-1) \text{ if } k \rightarrow 0. \quad (10)$$

### Fermi-Watson theorem

Below the two-pion threshold the excited nucleon can only decay by emitting a photon or a pion. The S-matrix then takes the general unitary form:

$$S = \begin{pmatrix} S_{\pi\pi} & S_{\gamma\pi} \\ S_{\pi\gamma} & S_{\gamma\gamma} \end{pmatrix} = \begin{pmatrix} \sqrt{1-\eta^2} e^{2i\delta_{\pi N}} & i\eta e^{i(\delta_{\pi N}+\delta_{\gamma N})} \\ i\eta e^{i(\delta_{\pi N}+\delta_{\gamma N})} & \sqrt{1-\eta^2} e^{2i\delta_{\gamma N}} \end{pmatrix}, \quad (11)$$

where the real number  $\eta$  is the inelasticity, and  $\delta_{\pi N}$  and  $\delta_{\gamma N}$  are the pion-nucleon and Compton scattering phases, respectively. Since the electromagnetic interaction is small, we may neglect the terms of order  $\eta^2$ . These approximations lead to the following T-matrix elements:  $T_{\pi\pi} = \sin \delta_{\pi N} e^{i\delta_{\pi N}}$ ,  $T_{\gamma\pi} = \pm e^{i\delta_{\pi N}} |T_{\gamma\pi}|$ , and  $T_{\gamma\gamma} = 0$ . Because the transition matrix element  $T_{\gamma\pi}$  is proportional to the electromagnetic multipoles of Eq. (7),  $T_{\gamma\pi} = \sqrt{2q(W)k(W, Q^2)} \mathcal{M}$ , also the electromagnetic multipoles carry the phase of the respective pion-nucleon states, for example,  $\mathcal{M}_{1+}^{3/2}(W, Q^2) = \pm e^{i\delta_{1+}^{3/2}(W)} |\mathcal{M}_{1+}^{3/2}(W, Q^2)|$ .

### Form factors

We restrict the following discussion to the  $\Delta(1232)$  resonance. Generalizations to higher resonances have been given, but the definitions become more involved. Corresponding to the independent transition multipoles, the following three form factors for the N- $\Delta$  transition can be defined:

$$\begin{aligned} M_{1+}^{3/2}(M_\Delta, Q^2) &= iN \frac{k_\Delta(Q^2)}{M_N} G_M^*(Q^2) \\ E_{1+}^{3/2}(M_\Delta, Q^2) &= -iN \frac{k_\Delta(Q^2)}{M_N} G_E^*(Q^2) \\ S_{1+}^{3/2}(M_\Delta, Q^2) &= -iN \frac{k_\Delta(Q^2)^2}{2M_N M_\Delta} G_C^*(Q^2), \end{aligned} \quad (12)$$

with  $N = \sqrt{3\alpha/(8q_\Delta\Gamma_\Delta)}$ , where  $\alpha \approx 1/137$ , and the photon ( $k_\Delta$ ) and pion ( $q_\Delta$ ) three-momenta have been evaluated at the resonance. The proportionality factor contains kinematics that relates pion photoproduction to total photoabsorption at the resonance. Comparing with Eq. (9) we note that these definitions divide out the  $k$  dependence at pseudothreshold such that the form factors are finite at this point. Equation (12) corresponds to the definition of Ash [4], the form factors of Jones and Scadron [5] are obtained by multiplication with an additional factor,  $G^{JS} = \sqrt{1+Q^2/(M_N+M_\Delta)^2} G^{Ash}$ .

### DYNAMIC MODELS

A dynamic model in the  $\Delta(1232)$  region contains the Hilbert vectors  $|N\pi\rangle$ ,  $|N\gamma\rangle$ , and  $|\Delta(1232)\rangle$ . The first step is to calculate the pion-nucleon scattering states, in a second step we include the electromagnetic interaction of the real or virtual photons with the pions and nucleons. A good introduction to this topic is given by Ref. [6], which also includes references to earlier work and a useful summary on various multi-channel K-matrix models that are needed to describe the higher energy region with many open channels.

## The pion-nucleon system

Dynamic models treat the hadronic system on the basis of a free hamiltonian, a quasi-potential, and "bare" transition operators describing the excitation of resonances. This hamiltonian is treated in the framework of a Bethe-Salpeter equation with the result of a fully unitary T-matrix, see, for example, Refs. [7, 8]. However, the quasi-potential does not allow the (virtual) production of heavier mass systems, for example, two-pion intermediate states are excluded. As a consequence, the model is not truly relativistic, even if the kinematics is relativistic. The quasi-potential  $v(\pi N \rightarrow \pi N) = v_{\pi N}$  describes a non-resonant background and is typically given by s- and u-channel Born terms and t-channel meson exchange. The  $t$ -matrix for the background takes the form

$$t_{\pi N}(W) = v_{\pi N}[1 + g_{\pi N}(W)t_{\pi N}(W)], \quad (13)$$

where  $g_{\pi N}$  is the propagator of the free pion-nucleon system. The background modifies the "bare" transition operator  $\Gamma_{\pi N \rightarrow \Delta}$ , which leads to the "dressed"  $N\Delta$  vertex

$$\tilde{\Gamma}_{\pi N \rightarrow \Delta}(W) = \Gamma_{\pi N \rightarrow \Delta}[1 + g_{\pi N}(W)t_{\pi N}(W)], \quad (14)$$

as well as the free  $\Delta$  propagator  $G_\Delta$ , which builds up the "dressed"  $N\Delta$  propagator

$$\tilde{G}_\Delta(W) = G_\Delta(W)[1 + \Sigma_\Delta(W)\tilde{G}_\Delta(W)] = [W - M_\Delta - \Sigma_\Delta(W)]^{-1}, \quad (15)$$

with  $\Sigma_\Delta$  the complex self-energy due to intermediate pion-nucleon loops. With these definitions the full T-matrix for pion-nucleon scattering takes the form

$$T_{\pi N}(W) = t_{\pi N}(W) + \tilde{\Gamma}_{\Delta \rightarrow \pi N}(W)\tilde{G}_\Delta(W)\tilde{\Gamma}_{\pi N \rightarrow \Delta}(W). \quad (16)$$

This Bethe-Salpeter equation is solved for each multipole ( $l\pm$ ) and isospin ( $I$ ) channel, and the parameters contained in both quasi-potential and bare  $\pi N \rightarrow \Delta$  vertex are fitted to the experimental pion-nucleon phase shifts  $\delta_{l\pm}^I(W)$ .

## The electromagnetic interaction

If the photon is absorbed by the target nucleon, it will either produce a pion-nucleon state by the transition potential  $v_{\gamma N \rightarrow \pi N}$  or a resonance by the bare vertex  $\Gamma_{\gamma N \rightarrow \Delta}$ . The electromagnetic background radiation is described by

$$t_{\gamma N \rightarrow \pi N}(W, Q^2) = v_{\gamma N \rightarrow \pi N}(W, Q^2) + t_{\pi N}(W)g_{\pi N}(W)v_{\gamma N \rightarrow \pi N}(W, Q^2). \quad (17)$$

The second term on the r.h.s of this equation describes the rescattering, to lowest order a pion-nucleon loop. The electromagnetic interaction excites the hadronic system to a virtual state with energy  $W'$ , which propagates with  $g_{\pi N}(W) = (W - W' + i\varepsilon)^{-1} = -i\pi\delta(W - W') + \mathcal{P}(W - W')^{-1}$ . This splits the rescattering term in on-shell and off-shell contributions, the latter ones being described by a principal value integral over all pion-nucleon scattering states with energy  $W'$ . A cautionary remark: In the work of Sato and Lee [7, 8] the rescattering in Eq. (17) is due to the non-resonant pion-nucleon interaction, that is, with the resonance switched off. In contrast, the DMT model [9, 10] uses the full pion-nucleon interaction in this equation.

The potential  $v_{\gamma N \rightarrow \pi N}$  is given by the s- and u-channel pion-nucleon Born terms, the Kroll-Ruderman term, and t-channel contributions from the exchange of neutral pions or vector mesons ( $\rho, \omega$ ). The meson-exchange diagrams contain some freedom, because the coupling between the mesons and the nucleon is not too well known. A further problem arises for the coupling of virtual photons. In principle, the s- and u-channel terms should appear with the Dirac and Pauli form factors of the nucleon, the Kroll-Ruderman term with the axial form factor of the nucleon, and the t-channel terms with pion or pion-meson transition form factors. However, a simple multiplication with the respective form factors violates gauge invariance. Instead, a consistent description requires that the form factors be built up from a gauge invariant many-body hamiltonian of the hadronic system, for example, in ChPT by loop diagrams to a given order of expansion. Short of a complete theory, one can either set all form factors equal, for example, to the familiar dipole form, or enforce gauge invariance explicitly by the replacement  $J_\mu \rightarrow J_\mu - k_\mu J \cdot k / k \cdot k$ . Although the latter procedure ensures gauge invariance, it is by no means unique. The bare vertex for the reaction  $\gamma + N \rightarrow \Delta$  can be

expressed by 3 transition form factors  $G_{M1}(Q^2)$ ,  $G_{E2}(Q^2)$ , and  $G_{C2}(Q^2)$ . The vertex becomes dressed by inserting all rescattering "bubbles",

$$\tilde{\Gamma}_{\gamma N \rightarrow \Delta}(W, Q^2) = \Gamma_{\gamma N \rightarrow \Delta}(Q^2) + \tilde{\Gamma}_{\pi N \rightarrow \Delta}(W, Q^2) g_{\pi N}(W) v_{\gamma\pi}(Q^2). \quad (18)$$

Combining these results we obtain the full  $T$ -matrix for the reaction  $\gamma + N \rightarrow \pi + N'$ ,

$$T_{\gamma N \rightarrow \pi N}(W, Q^2) = t_{\gamma N \rightarrow \pi N}(W, Q^2) + \tilde{\Gamma}_{\Delta \rightarrow \pi N}(W) \frac{1}{W - M_\Delta - \Sigma_\Delta(W)} \tilde{\Gamma}_{\gamma N \rightarrow \Delta}(W, Q^2). \quad (19)$$

This is again the definition of Sato and Lee. In order to compensate for the different form of the background, the dressed vertex  $\tilde{\Gamma}_{\gamma N \rightarrow \Delta}$  in Eq. (19) has to be replaced by the bare vertex  $\Gamma_{\gamma N \rightarrow \Delta}$  in the DMT model.

We repeat that pion rescattering is treated by summing up all diagrams with an arbitrary number of pion-nucleon bubbles in the intermediate states. However, these loops require a phenomenological cut-off  $\Lambda_{\pi N}$  to regularize the integrals for large off-shell momenta. We note that the rescattering effects are contained in all of the functions on the r.h.s. of Eq. (19). Furthermore, the rescattering process will contain model-dependent off-shell effects, even if all the pion-nucleon phase shifts are correctly reproduced. Let us now summarize the model-dependencies and shortcomings of the state-of-the-art dynamic models:

- the choice of the quasi-potential  $v_{\pi N}$  of pion-nucleon scattering and the cut-off  $\Lambda_{\pi N}$  for regularization of the loop integrals,
- the coupling constants of the vector mesons to pions and nucleons,
- the bare vertices  $\Gamma_{\pi N \rightarrow \Delta}$  and  $\Gamma_{\gamma N \rightarrow \Delta}$  for  $\Delta(1232)$  production by pions and photons, respectively,
- the choice of the bare  $N\Delta(1232)$  transition form factors  $G_{M1}(Q^2)$ ,  $G_{E2}(Q^2)$ , and  $G_{C2}(Q^2)$  corresponding to the multipoles  $M_{1+}$ ,  $E_{1+}$ , and  $S_{1+}$ , respectively,
- the neglect of intermediate states other than pion-nucleon loops, and of such loops before the photon has been absorbed, and
- the treatment of backgrounds from u-channel  $\Delta$  excitation and higher resonances.

## Comparison of dynamic and other phenomenological models

### *Sato-Lee model*

Sato and Lee (S-L) derive their dynamic model from a lagrangian in all parts [7, 8], in particular also the bare vertex for the  $\gamma + N \rightarrow \Delta$  transition is based on an effective lagrangian. The electromagnetic background is constructed according to Eqs. (13) and (17), that is, the pion produced by the non-resonant electromagnetic background is rescattering with the non-resonant part of the pion-nucleon interaction. Therefore the background amplitude carries the slowly varying phase  $\delta_b(W)$  of the pion-nucleon background. The exact value of this phase is certainly somewhat model-dependent. As an example, in the work of Höhler [1] this phase slowly decreases from  $-19.5^\circ$  at pion production threshold to about  $-24^\circ$  at  $W = 1232$  MeV. The cut-off for the  $\pi N$  loop integrals has a dipole form,  $F(\vec{q}) = (1 + \vec{q}^2/\Lambda^2)^{-2}$  with  $\Lambda$  in the range of  $(690 \pm 50)$  MeV, which corresponds to an r.m.s radius of nearly 1 fm. If the  $\Delta(1232)$  is produced or annihilated, a form factor of similar range is applied. The regularization procedure is fixed by the strong interaction, no additional regularization factors are introduced in pion electroproduction.

### *DMT model*

The Dubna-Mainz-Taipei (DMT) dynamic model differs from the S-L model by parameterizing the  $\Delta$  contribution to the reaction  $\gamma N \rightarrow \pi N$  right away in the form [9, 10]

$$t_{\gamma N \rightarrow \pi N}^{\Delta, \lambda}(W, Q^2) = \mathcal{A}^{\Delta, \lambda}(Q^2) f_{\pi\Delta}(W) \frac{\Gamma_\Delta M_\Delta}{M_\Delta^2 - W^2 - iM_\Delta \Gamma_\Delta} f_{\gamma\Delta}^\lambda(W) e^{i\Phi_\Delta(W)}, \quad (20)$$

where  $\Phi_\Delta(W)$  corrects the phase of the Breit-Wigner form to the experimental pion-nucleon phase shift  $\delta_{33}(W) = \delta_{1+}^{3/2}(W)$  and  $\lambda$  stands for the electromagnetic multiplicities E, M, or S. The  $Q^2$  dependence of the transverse multipoles is parameterized as

$$\mathcal{A}^{\Delta,\lambda}(Q^2) = \mathcal{A}^{\Delta,\lambda}(0) \frac{k_\Delta(Q^2)}{k_\Delta(0)} (1 + \beta Q^2) e^{-\gamma Q^2} G_D(Q^2), \quad (21)$$

where  $G_D(Q^2) = (1 + Q^2/0.71\text{GeV}^2)^{-2}$  is the dipole form factor,  $\beta$  and  $\gamma$  are free parameters to be determined from the data, and the explicit factor  $k$  in front provides the correct behavior at pseudothreshold.

At variance with the S-L model, the DMT model describes both resonant and non-resonant electromagnetic amplitudes with the full pion-nucleon interaction, that is, both contributions carry the full phase  $\delta_{33}(W)$ . The convergence of the loop integrals is enforced by a dipole cut-off  $F(\vec{q}', \vec{q}) = [(\Lambda^2 + \vec{q}'^2)/(\Lambda^2 + \vec{q}^2)]^2$  at the vertex leading from an on-shell pion with momentum  $\vec{q}$  to an off-shell pion with momentum  $\vec{q}'$ , and the cut-off is  $\Lambda = 440$  MeV.

#### MAID model

The MAID model [11] uses the pion-nucleon scattering phases as input. The resonance contribution to pion electroproduction is parameterized as in Eq. (20), and the non-resonant term is treated in an on-shell approximation, i.e., the principle value integral of the loop contribution is dropped. The resulting background contribution to the reaction  $\gamma N \rightarrow \pi N$  takes the form

$$t_{\gamma N \rightarrow \pi N}^{bg,\alpha}(W, Q^2) \rightarrow (1 + iT_{\pi N \rightarrow \pi N}^\alpha) K_{\gamma N \rightarrow \pi N}^\alpha \rightarrow e^{i\delta_\alpha(W)} \cos \delta_\alpha(W) v_{\gamma N \rightarrow \pi N}^\alpha(W, Q^2), \quad (22)$$

where  $v_{\gamma N \rightarrow \pi N}^\alpha$  is the quasi-potential for the non-resonant background terms, and  $\alpha$  denotes the quantum numbers. The background includes the usual nucleon Born terms as well as pion and vector meson t-channel contributions. The pion-nucleon scattering is described by a mixture of pseudovector (pv) and pseudoscalar (ps) couplings, such that the threshold scattering is purely pv as required by chiral invariance, whereas with increasing energy the interaction becomes more and more ps. The reason for this parameterization is that the additional gradient in pv coupling turns into a pion momentum and thus leads to an unphysical increase of the interaction for high energies, which in other models is damped by momentum-dependent form factors. We further point out that the ps and pv Born terms differ only in channels with total angular momentum  $J = 1/2$ , i.e., S wave (0+) and Roper (1-) multipoles.

#### Yerevan-JLab model

The ps-pv mixing in MAID was introduced in order to avoid cut-off form factors. As was pointed out by the Yerevan-JLab group [12], the original MAID model still showed a large increase of the Born terms at higher energies, which had to be compensated by unrealistically large resonance tails. It was therefore suggested to improve the MAID background by a gradual transition to the Regge behavior as function of  $s = W^2$ ,

$$t_{YL}^{bg,\alpha}(W, Q^2) = \frac{t_{MAID}^{bg,\alpha}(W, Q^2)}{1 + (s/s_{thr} - 1)^2} + \frac{(s/s_{thr} - 1)^2 t_{Regge}^{bg,\alpha}(W, Q^2)}{1 + (s/s_{thr} - 1)^2}, \quad (23)$$

with a Regge background containing the t-channel exchange of  $\pi, \rho, \omega, b_1$ , and  $a_2$  mesons. As is evident from Eq. (23), this description takes exactly the MAID value at threshold (pv coupling), but reduces the MAID background (a mixture of ps and pv coupling) to about 77 % in the  $\Delta$  resonance and 50 % in the second resonance region.

#### SAID parameterization

The SAID group parameterizes the world data in the form [13]

$$T^\alpha(W, Q^2) = [t_{Born}^\alpha(W, Q^2) + A^\alpha] [1 + iT_{\pi N}^\alpha(W)] + B^\alpha T_{\pi N}^\alpha(W) + (C^\alpha + iD^\alpha) [Im T_{\pi N}^\alpha(W) - |T_{\pi N}^\alpha(W)|^2]. \quad (24)$$

Since  $T_{\pi N} = \sin\delta_\alpha e^{i\delta_\alpha}$  below two-pion threshold, the first (background) term on the r.h.s. of Eq. (24) is proportional to  $\cos\delta_\alpha e^{i\delta_\alpha}$ , the second (resonant) term is proportional to  $\sin\delta_\alpha e^{i\delta_\alpha}$ , and the last term vanishes in this region of elastic scattering (except for small electromagnetic corrections). The functions A to D are fitted to the data in the form of a polynomial expansion in  $W$  and  $Q^2$ .

## RESULTS

In this section we compare the results of different approaches: the dynamic models of Sato and Lee (S-L, Ref. [7, 8]) and of the Dubna-Mainz-Taipei collaboration (DMT, Ref. [9, 10]), the effective field theories of Pascalutsa and Vanderhaeghen (P-V, " $\delta$ " expansion, Ref. [14]) and Gail and Hemmert (G-H, " $\varepsilon$ " expansion, Refs. [16, 15]), the phenomenological descriptions SAID [13] and MAID05 [11], and the work of Hanstein based on dispersion relations (DR, Ref. [2]). The basis of a comparison between theory and experiment are the multipoles, which are complex functions of  $W$  and  $Q^2$ . Apart from corrections due to isospin symmetry breaking and electromagnetic corrections, the Fermi-Watson theorem requires that all the  $\Delta$  multipoles  $\mathcal{M}^\alpha$  carry the phase  $\delta_{33}(W)$  in the energy range up to the  $\Delta$  region. As a consequence the real part of  $\mathcal{M}^\alpha$  vanishes at the  $K$ -matrix pole where  $\delta_{33}(W = M_\Delta) = 90^\circ$ . The PDG [3] lists  $M_\Delta = (1232 \pm 1)$  MeV, but the description of the data may improve by changing the pole position by several MeV. For example S-L has the pole at 1230.3 MeV, and for the listed SAID (SP06) solution the pole position is 1227.4 MeV for  $\pi^0$  kinematics and 1232.8 MeV for  $\pi^+$  kinematics. We further note that in the following text all values refer to the  $\Delta$  multipoles unless stated otherwise, and we have therefore dropped the isospin index  $I = 3/2$  in our notation.

### Delta(1232) multipoles at the K-matrix pole

Figure 1 shows the real and imaginary parts of the transverse  $\Delta$  multipoles for  $Q^2 = 0$  and the longitudinal multipole for  $Q^2 = 0.2 \text{ GeV}^2$  as function of  $W$ . The imaginary parts at the  $K$ -matrix pole are listed in Table 1 for a more quantitative discussion. The data points in Fig. 1 are obtained from the single-energy analysis of MAID05. There is general agreement among the different descriptions for the leading multipole  $M_{1+}$ , except that the curve S-L is slightly shifted to the lower energies, whereas the curve P-V is lower at the left and higher at the right shoulder of the resonance, which is probably due to the perturbative treatment of the background in the  $\delta$  expansion. Quite generally, the differences on both shoulders of the resonance are mainly due to different treatments of the backgrounds, not only of the non-resonant (3,3) background but also of other partial waves as  $E_{0+}^{(I)}$ ,  $M_{1-}^{(I)}$ ,  $E_{2-}^{(I)}$ , and so on. Therefore different models may see the data basis for the  $\Delta$  multipoles somewhat different, not so much for the leading magnetic transition but certainly for the much smaller electric and Coulomb transitions.

Seen in absolute values, the agreement is equally good for the multipole  $E_{1+}$ , however the differences become more visible because of the smallness of this multipole. The double zero in  $\mathcal{R}e(E_{1+})$  is remarkable, the first one is enforced by the Fermi-Watson theorem while the second one occurs because the large and negative non-resonant background takes over both below and above the resonance. The moderate differences for  $\mathcal{I}m(E_{1+})$  lead to large relative differences if this value is compared at the  $K$ -matrix pole  $W = M_\Delta \approx 1232$  MeV, as can be seen more quantitatively in Table 1. Because  $M_{1+}$  is pretty stable, it is convenient to compare the ratios  $R_{EM} = E_{1+}/M_{1+}$  and  $R_{SM} = S_{1+}/M_{1+}$  at the  $K$ -matrix pole. In this context it is worth pointing out that these ratios change rapidly as function of  $W$ : For example, within MAID and for  $Q^2 = 0$ ,  $R_{EM}$  increases from  $-7.5 \%$  at 1182 MeV and  $-2.2 \%$  at the  $K$ -matrix pole to  $+2.6 \%$  at 1282 MeV. The low value  $R_{EM} = -1.3 \%$  of SAID is obtained with the solution SP06 and  $\pi^0$  kinematics, earlier fits [13] yielded  $R_{EM} = -1.79 \%$  at  $Q^2 = 0$ . Because the multipoles are not yet available for the  $\varepsilon$  expansion of G-H [16], we have calculated them from the complex form factors by means of Eq. (12). Because of the perturbative approach in that reference, the ratios  $R_{EM}$  and  $R_{SM}$  become complex numbers indicating a strongly non-unitary result. The ratios are therefore listed in Table 1 with the definition of the authors,  $R_{EM} = \mathcal{R}e[E_{1+}/M_{1+}]$  etc., which of course in a unitary theory is identical with our definition but neglects the huge imaginary part in the non-unitary theory. More specifically, the phase at the  $K$ -matrix pole should be  $90^\circ$  for each multipole, whereas the multipoles of G-H have the phases  $83^\circ(M_{1+})$ ,  $-170^\circ(E_{1+})$ , and  $-146^\circ(S_{1+})$ . Moreover, the neglected imaginary part of the ratio  $R_{EM}$  is more than three times the real part shown in Table 1. We therefore suggest to fit the LECs to the behavior at the  $T$ -matrix pole and not at the  $K$ -matrix pole (see below).

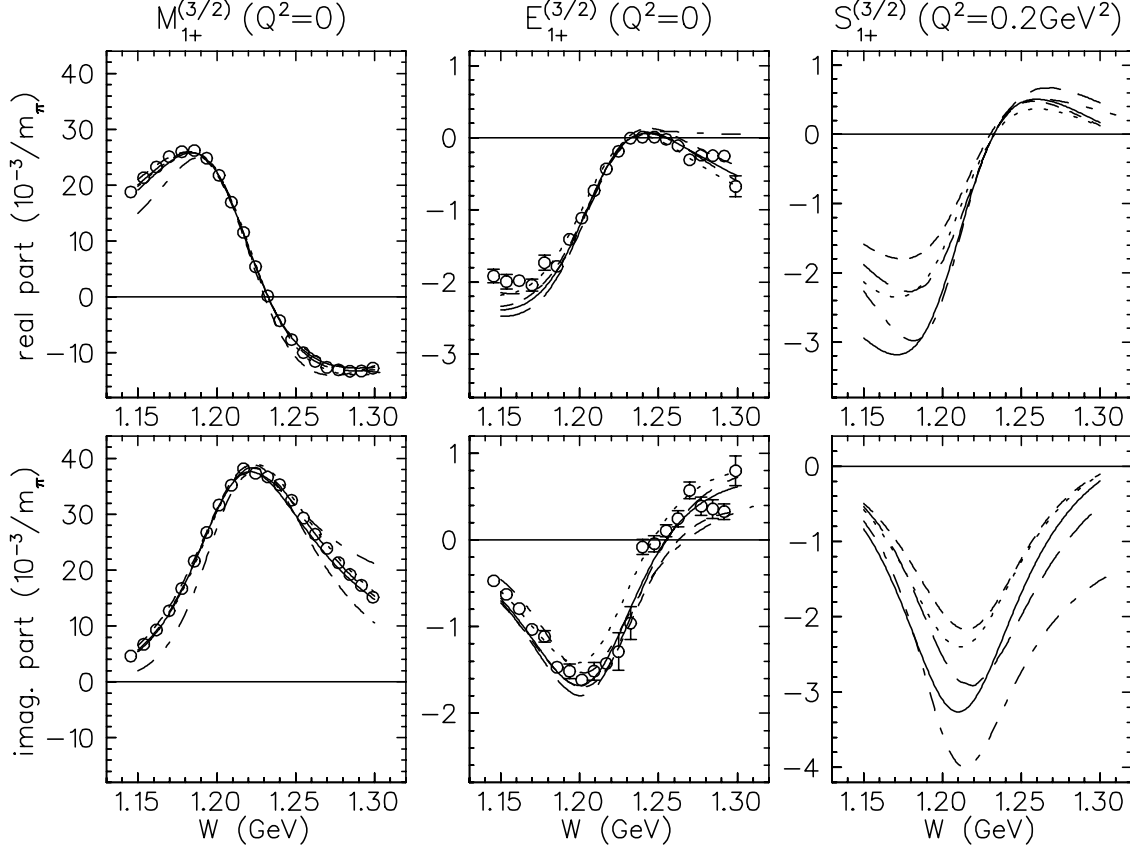


**FIGURE 1.** The real and imaginary parts of the multipoles  $M_{1+}^{(3/2)}$ ,  $E_{1+}^{(3/2)}$ , and  $S_{1+}^{(3/2)}$  as function of the c.m. energy  $W$ . The multipoles are in units of  $10^{-3}/m_{\pi^+}$ . Solid line: MAID05 [11], long-dashed line: DMT [9, 10], short-dashed line: S-L [7, 8], dashed-dotted line: P-V [14], dotted line: SAID(SP06) [13] for  $n\pi^+$  kinematics. The data are represented by the single energy solution of MAID05.

**TABLE 1.** The imaginary parts of the multipoles  $M_{1+}^{(3/2)}$ ,  $E_{1+}^{(3/2)}$ , and  $S_{1+}^{(3/2)}$  as well as the ratios  $R_{EM}$  and  $R_{SM}$  at the  $K$ -matrix pole for  $Q^2=0$  and  $0.2 \text{ GeV}^2$ . The multipoles are in units of  $10^{-3}/m_{\pi^+}$ .

	$M_{1+}$		$E_{1+}$		$S_{1+}$		$R_{EM} [\%]$		$R_{SM} [\%]$		references
$Q^2 [\text{GeV}^2]$	0	0.2	0	0.2	0	0.2	0	0.2	0	0.2	
S-L*	37.9	41.0	-1.03	-1.31	-0.88	-1.93	-2.7	-3.2	-2.3	-4.7	[7, 8]
DMT	37.2	39.7	-0.88	-1.13	-1.70	-2.59	-2.4	-2.8	-4.6	-6.5	[9, 10]
P-V	36.3	37.2	-0.83	-1.14	-1.28	-3.52	-2.3	-3.1	-3.5	-9.5	[14]
G-H <sup>†</sup>	36.5	37.1	-0.55	-0.36	-1.43	-2.43	-2.5	-1.8	-4.6	-6.9	[16]
SAID**	37.1	39.8	-0.47	-0.37	-1.54	-2.04	-1.3	-0.9	-4.2	-5.1	[13]
MAID	36.0	39.0	-0.78	-0.79	-2.38	-2.58	-2.2	-2.0	-6.6	-6.6	[11]
DR	37.9		-0.89				-2.4				[2]

\* pole at 1230.3 MeV

<sup>†</sup> imaginary parts of multipoles and real parts of the ratios of multipoles, as obtained from the complex form factors

\*\* solution SP06,  $p\pi^0$  kinematics

A view at the Coulomb multipole  $S_{1+}$  in Fig. 1 and Table 1 shows that the model predictions differ by up to a factor of two. In fact we have chosen  $Q^2 = 0.2 \text{ GeV}^2$  in the figure, because the comparison at  $Q^2 = 0$  looks even worse. Of course, this multipole can never be measured at the real photon point, but the recent experiments of the Bates/Mainz Collaboration at small values of  $Q^2$  down to  $0.05 \text{ GeV}^2$  will certainly lead to a convergence of the models, which partly differ because of lower, now withdrawn or corrected data points near  $Q^2 = 0.12 \text{ GeV}^2$ . Another (mild) constraint is the pseudo-threshold relation, Eq. (9), requiring  $S_{1+}$  to vanish at  $Q^2 = -0.086 \text{ GeV}^2$  with a curvature related to the slope of  $E_{1+}$ . In this context we repeat that gauge invariance yields the relation  $L_{1+}(Q^2 = 0) = S_{1+}(Q^2 = 0)$ , whereas the relation  $E_{1+} = L_{1+}$  is only valid at pseudothreshold.

The dependence of the multipoles on momentum transfer  $Q^2$  is shown in Fig. 2. The results for  $\mathcal{I}m(M_{1+})$  are reasonably well reproduced by all authors. We note that the decrease towards  $Q^2 = 0$  is enforced by the proportionality of  $M_{1+}$  with  $k$  near pseudothreshold,  $Q^2 = -0.086 \text{ GeV}^2$ . In the same limit, the ratio  $R_{EM}$  approaches a constant, whereas  $R_{SM}$  has to vanish. We observe that the different approaches yield quite different values for both  $R_{EM}$  and  $R_{SM}$ , but we repeat that also the data evaluation may depend on the backgrounds, which differ to some extent from model to model.

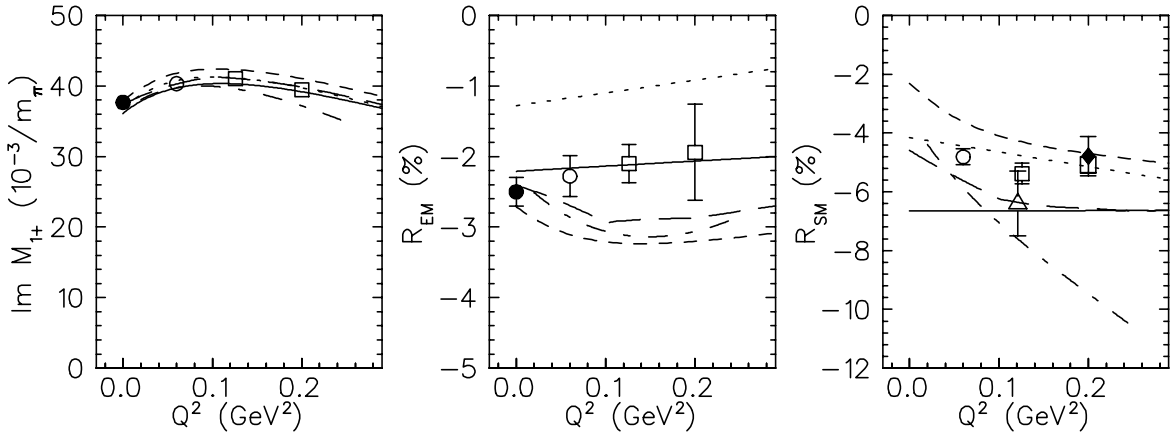


**FIGURE 2.** The imaginary part of the multipole  $M_{1+}^{(3/2)}$  and the ratios  $R_{EM}$  and  $R_{SM}$  at the  $K$ -matrix pole as function of  $Q^2$ . The multipole is given in units of  $10^{-3}/m_{\pi^+}$ , the ratios in %. Solid line: MAID05 [11], long-dashed line: DMT [9, 10], short-dashed line: S-L [7, 8], dashed-dotted line: P-V [14], dotted line: SAID (SP06) [13] for  $p\pi^0$  kinematics. The experimental data are from Refs. [17] (full circle), [18] (open circle), [19] (open triangle), [20] (open squares), and [21] (full diamond).

## Delta(1232) multipoles at the T-matrix pole

In this subsection we study the resonance structure of the different approaches: the position of the resonance pole in the complex  $W$  plane, the size of the resonance contribution at the pole, and the angle by which the non-resonant background rotates the phase of the resonance amplitude. Using the described speed plot technique and averaging over the results of the groups listed in Table 2, we find from the multipole  $M_{1+}$  and for  $Q^2 = 0$  the pole position at  $W = M_R - i\Gamma_R/2$ , with  $M_R = (1212 \pm 4) \text{ MeV}$  and  $\Gamma_R = (101 \pm 10) \text{ MeV}$ . The width obtained from the  $\delta$  expansion [14] is only 81 MeV and well below the  $1\text{-}\sigma$  range. We may attribute this small width to the perturbative treatment of the EFT, which should of course improve by going to higher order in the expansion. If we exclude this information from the average, the errors decrease by a factor of about two. The obtained values for the pole position compare well with the results from pion-nucleon scattering,  $(1210 \pm 1) \text{ MeV}$  for the real part and  $(100 \pm 2) \text{ MeV}$  for the width [3]. Quite similar results are obtained from the 2 other multipoles and as function of  $Q^2$ . The pole parameters  $Z_{M1+}$  obtained by the different approaches are listed in Table 2 for  $Q^2 = 0$  and  $0.2 \text{ GeV}^2$ . As average of the modulus we obtain  $r_{M1+} = (20.9 \pm 1.3) 10^{-3}/m_{\pi^+}$ . The average phase of the residue is  $\Phi_{M1+} = (-26.4 \pm 11.0)^\circ$ . This number is in the same ballpark as the background phase given by Höhler [1],  $-24^\circ$ , and about half of the corresponding phase in pion-nucleon scattering,  $-47^\circ$  [3]. The results for the small quadrupole transition are  $r_{E1+} = (1.21 \pm 0.12) 10^{-3}/m_{\pi^+}$  and  $\Phi_{E1+} = (-155 \pm 8)^\circ$ . From this we obtain the ratio  $r_{E1+}/r_{M1+} = (5.8 \pm 1.0) \%$  or, if we exclude Ref. [14] again, we have  $r_{E1+}/r_{M1+} = (5.8 \pm 0.5) \%$ . The small deviation of less than 10 % contrasts with the ratio at the

$K$ -matrix pole, which is much more model-dependent (see Table 1). These findings agree with earlier work [2, 22] showing that the ratio  $R_{EM}$  is more stable at the  $T$ -matrix pole than at the  $K$ -matrix pole. Similar to the situation at the  $K$ -matrix pole, the deviations for  $S_{1+}$  are much larger,  $r_{S1+} = (1.15 \pm 0.45)10^{-3}/m_{\pi+}$  and  $\Phi_{S1+} = (-177 \pm 23)^\circ$ .

**TABLE 2.** The strength of the multipole  $M_{1+}^{(3/2)}$ , as described by the resonance pole parameter  $Z_{M1+}$  according to Eq. (6), and the ratios  $R_{EM}^{pole}$  and  $R_{SM}^{pole}$  at the  $T$ -matrix pole for  $Q^2=0$  and  $0.2 \text{ GeV}^2$ .

	$Z_{M1+} [10^{-3}/m_{\pi+}]$		$R_{EM}^{pole} [\%]$		$R_{SM}^{pole} [\%]$		references
$Q^2 [\text{GeV}^2]$	0	0.2	0	0.2	0	0.2	
S-L*	21.9-4.7 i	24.1-3.7 i	-4.3-3.3 i	-4.0-2.3 i	-3.2-2.7 i	-5.3-1.7 i	[7, 8]
DMT	19.3-8.5 i	21.0-8.3 i	-3.8-5.3 i	-3.9-3.4 i	-4.9-3.8 i	-7.6-2.1 i	[9, 10]
P-V	12.9-13.2 i	14.8-13.1 i	-3.0-4.5 i	-3.0-4.3 i	-3.8-3.2 i	-9.6-1.9 i	[14]
SAID†	18.6-9.7 i	20.7-9.0 i	-2.8-4.8 i	-2.0-3.4 i	-3.5-0.2 i	-5.8-2.7 i	[13]
MAID	19.9-7.9 i	22.5-6.9 i	-3.7-4.4 i	-3.1-3.1 i	-7.5-4.5 i	-7.5-3.2 i	[11]
DR	18.8-9.8 i		-3.5-4.6 i				[2]

\*  $K$ -matrix pole at 1230.3 MeV

† solution SP06,  $n\pi^+$  kinematics

Finally, we compare these results with the  $\varepsilon$  expansion of Gellas *et al.* [15] who calculated the complex form factors for the decay  $\Delta \rightarrow N + \gamma$  in the framework of a chiral EFT. Since this work dresses the  $\Delta$  by pion-nucleon and pion- $\Delta$  loops but neglects the possibility of producing a non-resonant pion-nucleon system at the energy of the  $\Delta$ , it should be related to the situation at the  $T$ -matrix pole. And indeed, one obtains  $r_{E1+}/r_{M1+} = (5.8 \pm 0.2) \%$  from this reference, in agreement with the result presented above. However, the angles  $\Phi_{E1+}$  and  $\Phi_{M1+}$  differ from our findings, in particular  $\Phi_{E1+}$  is rotated by about  $100^\circ$  against our solution. Qualitatively similar results are obtained in the recent work of Ref. [16] except that the ratio  $r_{E1+}/r_{M1+}$  increases to 8.4 %.

## Quark bag vs. pion cloud physics

Figure 3 compares the full multipoles at the  $K$ -matrix pole with the corresponding results for the "bare"  $\Delta$ , and in Table 3 we list the values of the three  $\Delta$  multipoles as well as the ratios  $R_{EM}$  and  $R_{SM}$  for  $Q^2 = 0$  and  $Q^2 = 0.2 \text{ GeV}^2$ . The multipoles are plotted as function of  $Q^2$  in the range from the real photon point to a virtuality of  $1 \text{ GeV}^2$ . The pion rescattering or "pion cloud" contribution is quite substantial, as can be seen from the region between the respective dashed and dashed-dotted lines in Fig. 3. In the case of the magnetic dipole transition at  $Q^2 = 0.2 \text{ GeV}^2$ , the "bare" amplitude  $M_{1+}$  contributes only 70 % (S-L) or 60 % (DMT) to the full amplitude, that is, the pion cloud yields about one third of the transition strength. This explains why quark models chronically underestimate the  $M1$  transition by this amount. The figure also shows that the pionic contribution drops from about 1/3 of the total amplitude at the maximum to about 1/4 at  $Q^2 = 1 \text{ GeV}^2$ . In other words, the long-range physics drops out faster with increasing resolution due a typical radius of, say, 1 fm for the pion cloud, whereas the short-distance physics with a typical quark-bag of radius 0.5 fm decreases slower as function of  $Q^2$ . The two models differ more strongly for the electric and Coulomb multipoles. In particular the bare  $\Delta$  contribution to  $E_{1+}$  is negligible for the DMT model, whereas the S-L model obtains a 30 % contribution from the bare  $\Delta$ . Since both models describe the data reasonably well, we may ask what is the physical reason for this difference.

As we have seen before, the decomposition of "background" vs. "resonant" contributions is handled differently in the two models. In the DMT model, the background contribution refers to the non-resonant production of a pion ("the photon interacts initially with the pion cloud"), which after its production is re-scattered by the full hadronic interaction corresponding to the phase  $\delta_{33}$ . We can discuss this aspect more quantitatively by speed-plotting the two contributions for the DMT model. At  $Q^2 = 0$  we find the tiny ratio  $R_{EM}^{pole} = (0.2 + 0.2i) \%$  for the bare  $\Delta$ , which is to be compared with the value  $R_{EM}^{pole} = (-3.8 - 5.3i) \%$  for the full DMT model given in Table 2. Therefore the "background" contribution of the DMT model is essentially responsible for the residues of the small multipoles  $E_{1+}$  and  $S_{1+}$  at the  $T$ -matrix pole. In contrast, the slowly changing phase  $\delta_b$  appearing in the background term of the S-L model does not give rise to a pole with the properties of the  $\Delta$ , and as a consequence the residues of the electric and Coulomb strengths can not be provided by the background term of the S-L model. And indeed, the large effect

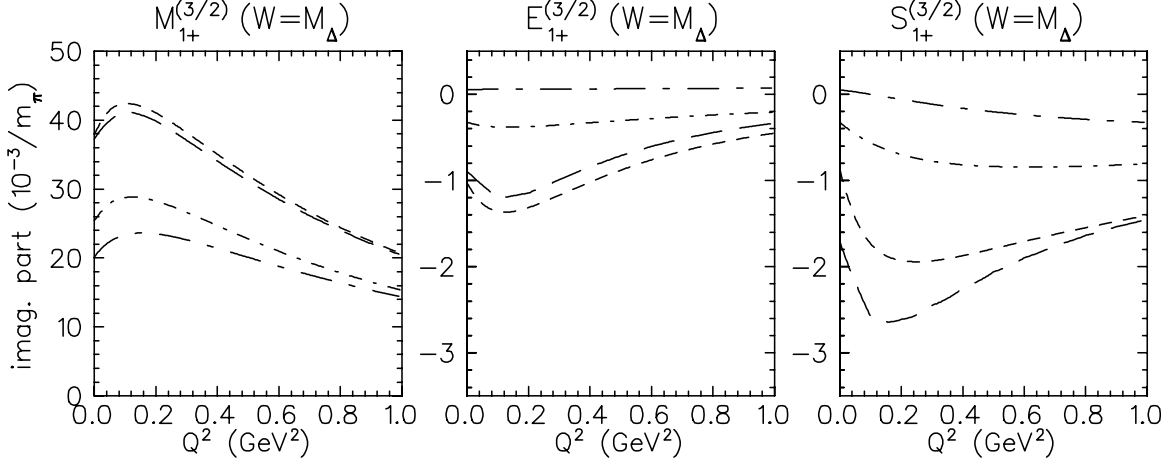


**FIGURE 3.** The imaginary parts of the multipoles  $M_{1+}^{(3/2)}$ ,  $E_{1+}^{(3/2)}$ , and  $S_{1+}^{(3/2)}$  at the K-matrix pole as function of  $Q^2$ . The multipoles are given in units of  $10^{-3}/m_{\pi}$ . Short-dashed line: S-L [7, 8], short-dashed-dotted line: S-L with the bare  $\Delta$  contribution only, long-dashed line: DMT [9, 10], long-dashed-dotted line: DMT with the bare  $\Delta$  contribution only.

of non-resonant pion production followed by  $\Delta$  excitation via rescattering, as observed in the DMT model, is now absorbed in the renormalization of the  $\gamma + N \rightarrow \Delta$  vertex of the S-L model. Of course, the different definitions do not explain why the "bare  $\Delta$ " contribution differs so much in the two models. However, the huge effect of  $\Delta$  production by rescattering may possibly give us some hint. Whereas the on-shell contribution of the rescattering term should be essentially model-independent, the principal value integral contains off-shell kinematics and therefore is very sensitive to model assumptions. In order to fully understand the issue, it would be interesting to compare the off-shell properties of the hadronic interaction in the two models and the resulting consequences for the bare  $\Delta$  vs. pion cloud contributions.

**TABLE 3.** The imaginary parts of the multipoles  $M_{1+}^{(3/2)}$ ,  $E_{1+}^{(3/2)}$ , and  $S_{1+}^{(3/2)}$  as well as the ratios  $R_{EM}$  and  $R_{SM}$  at the K-matrix pole for  $Q^2=0$  and  $0.2 \text{ GeV}^2$ . The multipoles are in units of  $10^{-3}/m_{\pi}$ . The results for the full 33-partial waves are listed in the upper row for each reference, the values for the bare  $\Delta$  resonance are in the lower row.

	$M_{1+}$		$E_{1+}$		$S_{1+}$		$R_{EM} [\%]$		$R_{SM} [\%]$		references
$Q^2 [\text{GeV}^2]$	0	0.2	0	0.2	0	0.2	0	0.2	0	0.2	
S-L full*	37.9	41.0	-1.03	-1.31	-0.88	-1.93	-2.7	-3.2	-2.3	-4.7	[7, 8]
bare	25.4	28.3	-0.33	-0.38	-0.32	-0.70	-1.3	-1.3	-1.3	-2.5	
DMT full	37.1	39.7	-0.87	-1.12	-1.51	-2.64	-2.3	-2.8	-4.1	-6.7	[9, 10]
bare	20.2	23.5	0.05	0.06	0.05	-0.06	0.3	0.3	0.3	-0.3	
G-H full†	36.5	37.1	-0.55	-0.36	-1.43	-2.43	-2.5	-1.8	-4.6	-6.9	[16]
bare	49.3		1.34		0.47						

\* pole at 1230.3 MeV

† imaginary parts of multipoles as obtained from the real part of the complex form factors

Let us now compare the results of the dynamic models with the  $\varepsilon$  expansion of Ref. [16], which splits the short-distance physics and the pion-cloud contribution at a scale of 1 GeV. The entry G-H in Table 3 shows that the pion cloud yields a negative contribution to  $M_{1+}$ , at variance with the dynamic models, which predict a positive contribution to the magnetic transition. As a consequence the fit to the data requires a "bare"  $\Delta$  form factor much above the data. This contradicts the common belief that the constituent quark models can be brought to agree with the data by including the pionic degrees of freedom. In the case of  $E_{1+}$ , the pionic contribution of the  $\varepsilon$  expansion is 2-3 times larger than predicted by the dynamic models, which requires a large cancelation with the short-distance physics. The same cancelation occurs also for  $S_{1+}$ , but to a lesser degree. In conclusion all approaches agree that the transverse electric and Coulomb N- $\Delta$  transitions are essentially determined by the pion cloud. However, there remain

serious numerical contradictions among the different descriptions. In order to clarify this issue it will be important to compare at the level of the multipoles, because only these are directly related to the experiment. Since the multipoles fulfill the Fermi-Watson theorem in the  $\Delta$  region, their ratios are real numbers, which is not the case for the form factors of Refs. [15, 16]. Therefore we suspect that some of the differences are due to the (partial) neglect of final-state interactions, which are expected to affect the multipoles quite differently.

Another point requiring some common studies is the dependence of the "bare vs. dressed  $\Delta$ " issue on the cut-off of the loop integrals or the scale of the separation. Of course, we are aware of the fact that a "pion cloud" or "bare" and "dressed"  $\Delta$  resonances are not observables, but still the physics behind the mere  $S$ -matrix elements remains intriguing. However, the picture we have in mind about the nucleon - an interior region of valence quarks, glue, and quark-antiquark pairs surrounded by a pion cloud - does only make sense if different approaches agree at least semi-quantitatively under the same conditions, for example, at the same scale of regularization.

## ACKNOWLEDGMENTS

We are grateful for helpful suggestions and numerical input to R.A. Arndt, G.C. Gail, S.S. Kamalov, T.-S.H. Lee and T. Sato, V. Pascalutsa and M. Vanderhaeghen. This work was supported by the Deutsche Forschungsgemeinschaft (SFB 443).

## REFERENCES

1. G. Höhler and A. Schulte,  $\pi$ N Newsletter **7** 94 (1992); G. Höhler,  $\pi$ N Newsletter **9** 1 (1993).
2. O. Hanstein, D. Drechsel, and L. Tiator, Phys. Lett. B **385**, 45 (1996).
3. W.-M. Yao *et al.* (Particle Data Group), J. Phys. G **33**, 1 (2006).
4. W.W. Ash *et al.*, Phys. Lett. B **24**, 165 (1967).
5. H.F. Jones and M.D. Scadron, Annals Phys. **81**, 1 (1973).
6. V.D. Burkert and T.-S. H. Lee, Int. J. Mod. Phys. E **13**, 1035 (2004).
7. T. Sato and T.-S. H. Lee, Phys. Rev. C **54**, 2660 (1996).
8. T. Sato and T.-S. H. Lee, Phys. Rev. C **63**, 055201 (2001).
9. S.S. Kamalov and S.N. Yang, Phys. Rev. Lett. **83**, 4494 (1999).
10. S.S. Kamalov, S.N. Yang, D. Drechsel, O. Hanstein, and L. Tiator, Phys. Rev. C **64**, 032201 (2001).
11. D. Drechsel, O. Hanstein, S.S. Kamalov, and L. Tiator, Nucl. Phys. A **645**, 145 (1999).
12. I.G. Aznauryan, Phys. Rev. C **67**, 015209 (2003).
13. R.A. Arndt, W.J. Briscoe, J.J. Strakovsky, and R.L. Workman, Phys. Rev. C **66**, 055213 (2002).
14. V. Pascalutsa and M. Vanderhaeghen, Phys. Rev. Lett. **95**, 232001 (2005).
15. G.C. Gellas, T.R. Hemmert, C.N. Ktorides, and G.I. Poulis, Phys. Rev. D **60**, 054022 (1999).
16. T.A. Gail and T.R. Hemmert, nucl-th/0512082 (2005).
17. R. Beck *et al.*, Phys. Rev. Lett. **78**, 606 (1997) and Phys. Rev. C **61**, 035204 (2000).
18. S. Stave *et al.* (A1 Collaboration), nucl-ex/0604013 (2006).
19. Th. Pospischil *et al.*, Phys. Rev. Lett. **86**, 2959 (2001).
20. N.F. Sparveris *et al.*, Phys. Rev. Lett. **94**, 022003 (2005); *Proceedings of the Workshop on the Shape of Hadrons*, Athens, 2006.
21. D. Elsner *et al.* (A1 Collaboration), Eur. Phys. J. A **27**, 91 (2006).
22. R.L. Workman and R.A. Arndt, Phys. Rev. C **59**, 1810 (1999).

